

phys. stat. sol. (a) **169**, 171 (1998)

Subject classification: 78.20.Ci; 68.35.Dv; 72.40.+w; S11

Holographic Recording in Planar Cu:H:LiTaO₃ Waveguides

S.M. KOSTRITSKII (a) and D. KIP (b)

(a) *Physics Department, Kemerovo University, 650043 Kemerovo, Russia*
e-mail: root@chsb.kemgu.kemerovo.su; Fax: (+7) 3842525383

(b) *Fachbereich Physik, Universität Osnabrück, D-49069 Osnabrück, Germany*
e-mail: dkip@physik.uni-osnabrueck.de; Fax: (+49) 5419692670

(Received June 10, 1998; in revised form July 8, 1998)

Photorefractive planar waveguides in LiTaO₃ are fabricated by a proton exchange and a successive copper exchange from melts, containing either Cu⁺ or Cu²⁺ ions. The influence of different fabrication steps on refractive index profiles, hydrogen content, optical absorption, and waveguide transparency is investigated. With holographic methods dark and photoconductivity, holographic sensitivity, and light-induced refractive index change are measured. By the additional copper exchange the steady-state diffraction efficiency of holographic gratings in the waveguides is increased from 0.005 to 81%. Here the crucial influence of both, Cu valence state and hydrogen concentration on the holographic sensitivity is demonstrated.

1. Introduction

Recently the fabrication and investigation of photorefractive waveguides in proton-exchanged LiTaO₃ crystals has been reported [1,2]. The photorefractive properties of these waveguides were considerably improved by an additional copper exchange. Such nonlinear waveguides may be used as integrated optical switches, sensors, or memory cells [3]. Therefore, in the last few years the investigation of new fabrication methods of photorefractive waveguides has been considerably intensified. In the case of LiTaO₃ crystals the combined proton and copper exchange is a new method, which has clear advantages compared to other techniques [1,4,5]. Moreover, further improvement of Cu:H:LiTaO₃ waveguides should be possible by optimizing the fabrication conditions, because the quality of the waveguiding layer may be further improved by annealing treatments.

The formation of Cu:H:LiTaO₃ waveguides has been realized before [1,2,4] by a treatment of the proton-exchanged LiTaO₃ waveguides in melts prepared with copper acetate, where the copper in the melt exists mostly in form of Cu²⁺ ions. On the other hand, for the fabrication of Cu:H:LiNbO₃ waveguides both, the same melt [6,7] and melts prepared with Cu₂O [5,6,7], have been used. In the latter case, Cu is present in the state of Cu⁺ ions. The largest improvement of the photorefractive properties of Cu:H:LiNbO₃ waveguides has been obtained by the use of Cu₂O, because the photorefractive sensitivity is proportional to the ratio of Cu⁺/Cu²⁺ in the waveguiding layer. In this paper we report a new approach to increase the photorefractive sensitivity of Cu:H:LiTaO₃ waveguides by an optimization of the fabrication conditions.

Table 1

Waveguide notation and parameters of the Cu exchange of the investigated samples. The conditions of the proton exchange and the preliminary annealing are the same for all samples. BA, benzoic acid; LB, lithium benzoate; CO, copper oxide (Cu_2O); CA, copper acetate

sample	melt composition	temperature [$^{\circ}\text{C}$]	exchange [min]
H1	—	—	—
I-CuH1	BA + 0.84 mol% CO + 1.1 mol% LB	230	10
I-CuH2	BA + 0.84 mol% CO + 1.1 mol% LB	230	60
I-CuH3	BA + 2.5 mol% CO + 1.1 mol% LB	230	60
II-CuH1	BA + 7 wt% CA + 1.1 mol% LB	249	30
II-CuH2	BA + 7 wt% CA + 1.1 mol% LB	249	60
II-CuH3	BA + 7 wt% CA + 1.1 mol% LB	249	90

2. Waveguide Fabrication

For the fabrication of the waveguides we use polished z -cut LiTaO_3 substrates of nearly congruent melting composition. The substrates are subjected to the following treatments: 1. proton exchange in pure benzoic acid at 240°C for 8 h, 2. preliminary annealing in dry air at temperatures ranging from 265 to 350°C and for 45 to 285 min, 3. Cu exchange by two different methods: a) Cu(I) exchange in molten benzoic acid mixed with Cu_2O (from 0.84 to 2.5 mol%) at 230°C for 10 to 60 min. In some cases 1 to 2 mol% lithium benzoate (LB) is added to the mixture; b) Cu(II) exchange in molten benzoic acid mixed with 7 wt% copper acetate at 249°C for 30 to 90 min. In a last step (4) annealing in either dry air or argon atmosphere at 350°C for 1 to 16 h is performed. The fabrication parameters for some waveguides, whose properties will be discussed in more detail, are shown in Table 1. The conditions for the Cu(II) exchange are the same as in a previous study [1].

3. Waveguide Characterization

3.1 Content and valence state of Cu ions in the waveguides

The Cu content in the waveguides is determined by measuring the optical absorption of the samples in the UV and in the visible region with the help of a Cary 17D spectrometer. As can be seen in Fig. 1, depending on the method which has been used for Cu doping (fabrication step 3a or 3b, respectively), different changes in the optical spectrum are observed: the Cu(I) exchange (step 3a) induces a new band in the absorption spectrum at about 3.3 eV, which increases with the duration of the Cu exchange. Here the maximum value of optical density of the band is 0.18, which is reached after a treatment of the crystal for 60 min in a melt containing 2.5 mol% Cu_2O and 1 mol% lithium benzoate. On the other hand, the Cu(II) exchange (step 3b) induces another absorption band at about 4 eV. Its optical density ranges from 1 to 2.3 at a variation of the exchange duration from 30 to 90 min. A comparison with the optical spectrum of a volume-doped $\text{LiTaO}_3:\text{Cu}$ crystal allows to conclude, that the band at 3.3 eV is connected with Cu^+ ions, and the band at 4 eV is probably connected with Cu complexes.

We observe a strong transformation of the optical spectra of the Cu(II)-exchanged waveguides during the final annealing (step 4) that does not depend on the used atmo-

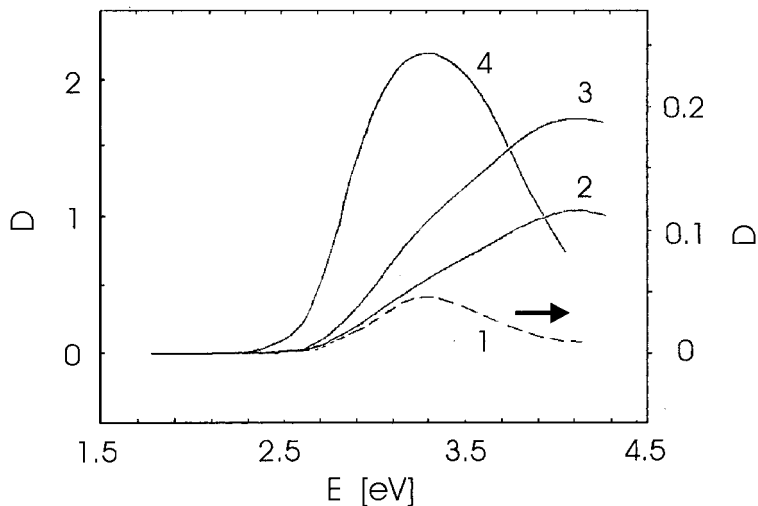


Fig. 1. Optical density D of different Cu-exchanged LiTaO₃ waveguides as a function of photon energy E . Curve 1, sample I-CuH3; curve 2, sample II-CuH1; curve 3, sample II-CuH2; curve 4, difference spectrum of a volume-doped LiTaO₃:Cu crystal ($C_{Cu} = 0.02$ mol%) and a nominally pure LiTaO₃ crystal

sphere: the new band at about 4 eV observed in the absorption spectrum becomes asymmetric, and the “center of gravity” shifts to higher energy, see Fig. 2. The intensity of this band decreases during annealing, and simultaneously the band at 4.2 eV that exists already in the undoped substrate [8] increases. Additionally, the analysis of the difference spectrum between non-annealed and annealed Cu(II)-exchanged waveguides shows the appearance of a weak band (optical density 0.01 to 0.02) at 3.3 eV that is created by annealing. Using data from [9] we find that in all Cu(II)-exchanged waveguides the Cu content is one to two orders of magnitude higher than in the Cu(I)-exchanged waveguides.

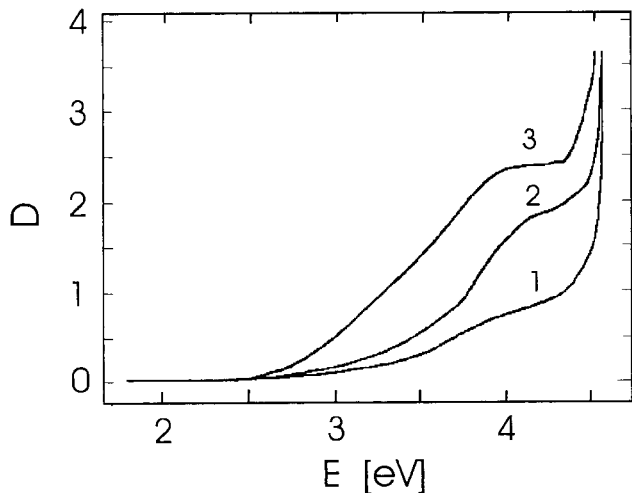


Fig. 2. Optical density D of different Cu-exchanged LiTaO₃ waveguides as a function of photon energy E . Curve 1, sample H1 (undoped); curve 2, sample II-CuH2 annealed for 16 h; curve 3, sample II-CuH2 before final annealing

3.2 Hydrogen content

IR spectra are measured with the help of a Specord M50 spectrometer in the frequency range of the OH stretching band around 3500 cm^{-1} to determine the hydrogen content in the waveguides. The intensity of the OH band is almost proportional to the hydrogen content [10]. Furthermore, this allows to determine the average value of proton exchange degree x for $\text{Li}_{1-x}\text{H}_x\text{TaO}_3$ layers, because the frequency and shape of the OH band depend clearly on x [10,11].

For Cu(I) exchange in melts that do not contain lithium benzoate (LB), the hydrogen content increases up to 25%, and a shift of the OH band towards higher frequencies of up to 6 cm^{-1} is observed. The latter points to a strong increase of the exchange degree x in the $\text{Li}_{1-x}\text{H}_x\text{TaO}_3$ waveguiding layer. However, these results are in contradiction to the weak changes in the hydrogen content (less than 3% for an exchange of 90 min) during the Cu(II) exchange, that are again in accordance with data of [4].

The increase of the exchange degree x leads to a reduction of the photorefractive effects in Cu:H:LiTaO₃ waveguides [1,2]. Therefore, we add some mol% LB to the mixture that is used for Cu(I) exchange, see Table 1. The addition of 1.1 mol% LB results in a frequency shift of the OH band of about 1.5 cm^{-1} , and the proton content increase has a small value of 7%. Furthermore, these results demonstrate the influence of copper acetate on the acidity of the benzoic acid used for proton exchange, that is similar to the well known influence of lithium benzoate [12].

3.3 Effective refractive indices

The effective refractive indices n_{eff} of the TM modes are measured by the method of prism coupling (dark line spectroscopy) at $\lambda = 514.5\text{ nm}$. From the set of n_{eff} the profile of the refractive index n_e is reconstructed with the use of an inverse WKB method. After annealing (step 4) for 1 to 16 h, in all samples five to seven TM modes can be excited, where the number of observed TM modes depends on annealing time [11]. The refractive index profiles have a nearly Gaussian form, and the refractive index increase Δn_e near the surface is significantly increased when compared with the initial stage after proton and Cu exchange. The magnitude of the increase of Δn_e grows (up to 0.017) with increasing Cu content in the Cu(II)-exchanged waveguides that are annealed for 1 h. However, this Cu-related increase decreases rapidly when the samples are further annealed, and for samples annealed for 16 h these values are lower than 0.005.

3.4 Waveguide transparency

The waveguide transparency is measured with the help of two rutile prisms which couple light of an argon ion laser ($\lambda = 514.5\text{ nm}$) into and out of the waveguide. The distance between the coupling points of these prisms is 4.5 mm. To obtain the absorption values the ratio of output to input power for the excitation of different modes is measured. A Cu exchange of both the Cu(I) and the Cu(II) type results in a decrease of the waveguide transparency, its size depending on the duration of Cu exchange and the Cu concentration in the melt. Therefore, the transparency of the heavily doped waveguides I-CuH3 and II-CuH3 is small, and such waveguides are not of practical interest for integrated-optical devices working in the green-violet spectral range.

The Cu-related decrease of transparency depends on the excited mode of the waveguide. A lower absorption is observed for modes with higher index, i.e., for modes that propagate closer to the surface. This dependence has a rather step-like behavior, as the characteristic depth of the Cu profile is small compared to the width of the refractive index profile. The annealing of the Cu-exchanged waveguides at 350 °C leads to a broader refractive index profile, and at the same time the depth where a marked Cu-related absorption is observed increases. This indicates the blurring of the initial Cu profile, that becomes essential for annealing times larger than 6 h. However, the precise determination of the Cu-related contribution to the decrease of the waveguide transparency, which is required for a Cu profile reconstruction, is not possible in this way, as other damping contributions connected with light scattering and substrate losses still exist. Moreover, the optical losses induced by light scattering do not change monotonously with an increase of the annealing time, as it is observed in undoped LiTaO₃ waveguides [1], however, they reach a minimum value for annealing for 16 h. This is an important advantage of strongly annealed waveguides.

The data of the waveguide transparency allow to determine the relative values of the Cu-related absorption when we compare different Cu-exchanged waveguides with the same degree of annealing. There is a significant difference between Cu(I)-exchanged and Cu(II)-exchanged waveguides, concerning changes of the Cu-related decrease of the waveguide transparency when changing the laser wavelength from 514.5 to 488 nm. A different ratio N of the magnitudes of the Cu-related absorption at 488 and 514.5 nm is measured: in the Cu(I)-exchanged waveguides we find $N = 2.6 \pm 0.5$, and for the Cu(II) exchange $N = 6.5 \pm 0.5$. After annealing of the Cu(II)-exchanged samples N decreases significantly. This change is observed simultaneously with the transformation of the optical spectra shown in Fig. 2. At the same time, in the Cu(I)-exchanged waveguides N keeps nearly constant for any annealing time. After annealing for a long time (16 h and more) the value of N of the Cu(II)-exchanged waveguides tends to that of the Cu(I)-exchanged waveguides. This points to the creation of single-charged Cu ions in the Cu(II)-exchanged waveguides, which seems to be caused by a dissociation of the Cu complexes during annealing.

4. Photorefractive Properties

4.1 Holographic methods

For the investigation of light-induced refractive index changes Δn , holographic gratings are written and erased by using an argon ion laser (wavelengths of 457.9, 488 and 514.5 nm). Two slightly focused beams are coupled into and out of the waveguide using two rutile prisms. Depending on the angle under which the light enters the prism, different extraordinarily polarized TM modes are excited. In the experimental set-up two modes intersect at an angle of $2\theta = 10^\circ$, and the interaction length l in the waveguides is about 1.5 mm. During the build-up of the refractive index grating, the diffraction efficiency η is measured as a function of time by blocking one of the beams for a short time (50 ms), and measuring the ratio of diffracted and total light intensity of the out-coupled beams. When the saturation value of the diffraction efficiency η^s is reached, one of the beams is switched off, and the continuous decrease of the diffracted light intensity indicates the decay of the grating during readout.

4.2 Saturation value of diffraction efficiency

In non-annealed (or in weakly annealed) waveguides, both undoped and Cu-doped, we do not observe holographic grating recording at any level of input power P_{in} (measured in front of the incoupling prism; the total coupling efficiency is about 1%) for all lines of the argon ion laser. However, after annealing either in air or argon atmosphere at 350 °C, effective writing of phase holograms becomes possible.

The behavior of η^s is well described by [13,14]

$$\eta^s = \exp(-\alpha l) \sin^2[(\pi \Delta n^s l)/(\lambda \cos(\Theta))], \quad (1)$$

where Δn^s is the steady-state value of light induced refractive index change, and α is the absorption coefficient. For low copper doping and a corresponding low Cu-related absorption, the diffraction efficiency increases monotonously with increasing input power P_{in} up to a maximum value η_{max}^s , see Fig. 3 (curve 2). Furthermore, the size of η_{max}^s correlates with the Cu content in the samples. For higher Cu doping and absorption coefficients, respectively, the value of η_{max}^s decreases again with growing Cu doping. Because of the spectral dependence of the Cu-related absorption this behavior is more pronounced for $\lambda = 488$ nm than for $\lambda = 514.5$ nm.

There is a certain threshold value P_{in}^t where the dependence $\eta^s(P_{in})$ changes qualitatively, i.e., at $P_{in} > P_{in}^t$ the value of η^s decreases with larger input power P_{in} . This behavior, which can be seen in Fig. 3 (curve 3), is a result of the photo-induced scattering or fanning of the guided light. The threshold value P_{in}^t is found to be inversely proportional to the Cu content and increases with larger hydrogen concentration. In most cases the maximum value η_{max}^s is observed at intermediate or low values of P_{in} , and in extreme cases fanning suppresses holographic recording at all. It has to be mentioned

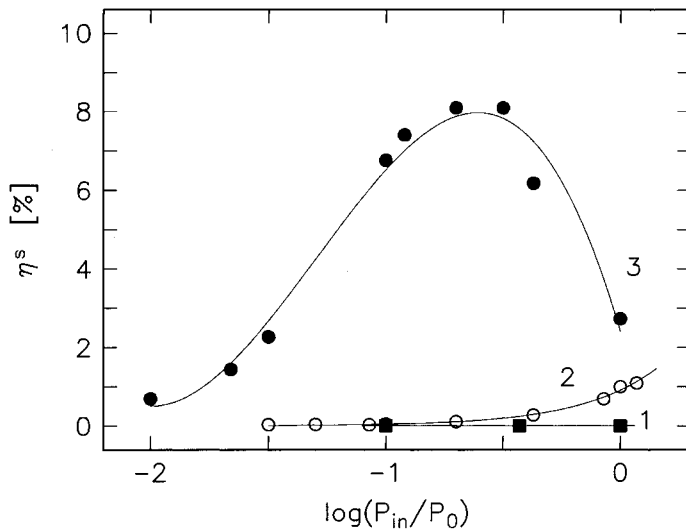


Fig. 3. Maximum value of diffraction efficiency η^s as a function of the normalized input power P_{in}/P_0 with $P_0 = 1$ W and at a wavelength of 514.5 nm. Curve 1, sample H1 (TM₄ modes) annealed for 1 h; curve 2, sample I-CuH1 (TM₃ modes) annealed for 6 h; curve 3, sample II-CuH1 (TM₃ modes) annealed for 6 h. The lines are merely guides for the eye

that there is a strong influence of a geometrical factor [15] on the fanning threshold, i.e., with increase of the aperture of the recording beams the light intensity I is reduced, and therewith the fanning threshold P_{in}^f increases significantly.

We observe significantly different values of η_{max}^s for different TM modes of the same sample. Earlier in [1], a crucial influence of the phase and composition of the waveguiding layer has been found that depends on the hydrogen concentration x at a depth d of the waveguiding layer, and the diffraction efficiency can be expressed as

$$\eta^s = (x_b - x)^2 (x_t - x)^2, \quad (2)$$

where $x_b \approx 0.6$ is the value for the lower boundary of a pure β -phase [11,12], and $x_t \approx 0.26$ is the threshold value for another phase transition, probably the upper limit of a pure α -phase. This influence of x plays a dominating role for the photorefractive properties of the waveguides, in particular for the samples annealed for less than 3 h [1,2]. Further annealing provides a decrease of x below the threshold of the above phase transitions for all TM modes.

From our data we can conclude that the dependence of Δn_s on input power P_{in} (in the absence of beam fanning) is clearly sublinear. This is in accordance with recent results obtained for proton-exchanged and annealed proton-exchanged LiTaO₃ [16,17] and LiNbO₃ [16,18] waveguides. In [18] it has been demonstrated that for large intensity I , photoconductivity is proportional to $I^{1/y}$, where $y > 1$, and thus $\Delta n^s \propto I^{(1-1/y)}$.

The largest improvement of the photorefractive properties of proton-exchanged waveguides is obtained using Cu(II) exchange: in the waveguide II-CuH1 (annealed for 16h) we obtain values from 2.7 to 18.1% for the steady-state diffraction efficiency and at a total input power from 40 to 230 mW. With the use of unfocused instead of focused recording beams we obtain a maximum value for η_{max}^s of 81%, see Fig. 4. Here holo-

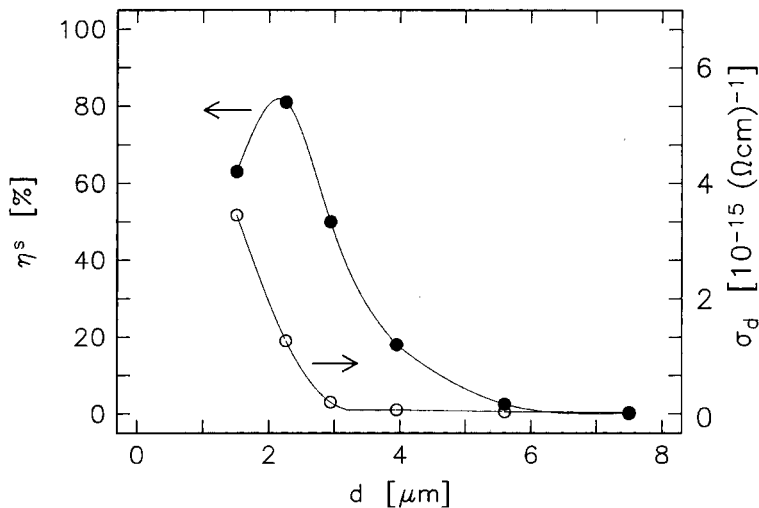


Fig. 4. Maximum value of diffraction efficiency η^s and dark conductivity σ_d as a function of the propagation depth d of the excited modes for the sample II-CuH1 annealed for 16h. The depth d is defined as the “center of gravity” of the corresponding intensity distribution. The wavelength is 514.5 nm and the input power is 20 mW. The lines are merely guides for the eye

graphic recording is possible without any beam fanning. Using Eq. (1) and an interaction length of $l = 1.5$ mm we get a light-induced extraordinary refractive index change of $\Delta n^s = 2.9 \times 10^{-3}$, a value that is much higher than for undoped proton-exchanged LiTaO₃ waveguides [16,17,19].

4.3 Kinetics of dark and photoerasure

From the time constants τ and τ_d of erasure with and without illumination we deduce the photo and dark conductivity, σ_{ph} and σ_d , using the relations $\sigma = \epsilon\epsilon_0/2\tau$, $\sigma_d = \epsilon\epsilon_0/2\tau_d$, and $\sigma = \sigma_{\text{ph}} + \sigma_d$, respectively. Both, dark and photo conductivity depend on the propagation depth d of the excited mode. Dark conductivity decreases with increasing annealing time, which may be related to the decreasing hydrogen concentration x during annealing, but σ_d is found to be not simply proportional to x . This may be connected with the influence of phase transitions of the waveguiding layer as described in [12].

A comparison of the values of τ_d and τ shows that dark and photoconductivity have similar values of some 10^{-15} to $10^{-13} (\Omega \text{ cm})^{-1}$ (for typical intensities in our experiments) in all samples, but photoconductivity still dominates. In some cases the high dark conductivity, which is observed in particular for the lowest modes of a waveguide, can result in a significant decrease of the maximum value of diffraction efficiency. As an example, this behavior is shown in Fig. 4 for the sample II-CuH1.

We deduce the photoconductivity σ_{ph} from the experimental data of τ and τ_d . Beam fanning limits these measurements to low input powers, where the light intensity I in the waveguide is proportional to P_{in} . Thus we can write

$$(\tau P_{\text{in}})^{-1} \propto \sigma_{\text{ph}}/P_{\text{in}} = a\sigma_{\text{spec}}I/P_{\text{in}}, \quad (3)$$

where σ_{spec} is the specific photoconductivity. When we split the absorption coefficient into two contributions, absorption of the undoped sample and absorption that is related to Cu doping, $a = a_{\text{u}} + a_{\text{Cu}}$, we can determine the relative changes of the Cu concentration c_{Cu} in the waveguide:

$$c_{\text{Cu}} = A_j a_{\text{Cu}} \propto (\tau_{\text{Cu}} P_{\text{in}})^{-1} - (\tau_{\text{u}} P_{\text{in}})^{-1}, \quad (4)$$

where τ_{Cu} and τ_{u} are the time constants for photoerasure in the Cu-doped and undoped waveguides, respectively. The coefficients A_j , $j = \text{I, II}$, are different for the Cu(I)- and Cu(II)-exchanged waveguides, $A_{\text{I}} \gg A_{\text{II}}$, and A_{II} increases with annealing time, while A_{I} keeps nearly constant.

From the measurement of photoerasure of the phase holograms recorded with different TM modes and using Eq. (4), we determine that the Cu profile in all Cu-exchanged waveguides has a nearly Gaussian form. We evaluate the diffusion constant D_{Cu} for the process of Cu exchange in proton-exchanged LiTaO₃ waveguides to be $D_{\text{Cu}}(\text{I}) = 0.35 \text{ mm}^2/\text{h}$ (without any LB) and $D_{\text{Cu}}(\text{II}) = 0.14 \text{ mm}^2/\text{h}$ for the Cu(I) and Cu(II) exchange, respectively. The distribution coefficient (i.e., the ratio between the Cu concentration in the waveguide and that in the melt) for the Cu(I)-exchanged waveguides is more than one order of magnitude smaller than for Cu(II)-exchanged waveguides. Furthermore, for strong annealing a significant blurring of the Cu profile is observed.

Table 2

Linear and quadratic part of holographic sensitivity, R_l and R_q (in $10^{-3}(\text{Ws})^{-1}$ and $10^{-3}(\text{W}^2\text{s})^{-1}$, respectively), and the inverse product $(\tau P_{\text{in}})^{-1}$ (in $10^{-3}(\text{Ws})^{-1}$) for different samples and the two wavelengths 488 and 514.5 nm. Here t_a is the time of annealing (in h). In some cases that are denoted with an asterix strong beam fanning occurs

sample	t_a	modes	$\lambda = 488 \text{ nm}$			$\lambda = 514.5 \text{ nm}$		
			R_l	R_q	$(\tau P_{\text{in}})^{-1}$	R_l	R_q	$(\tau P_{\text{in}})^{-1}$
H1	3	TM ₃	0.35	0	4.0	<0.1	0	≈0.3
I-CuH1	3	TM ₃	5.2	0.19	43	1.6	0.07	16.5
	6	TM ₃	1.4	0.05	15	0.72	0.03	9.5
I-CuH2	6	TM ₃	6.5	0.32	210	19	1.0	145
II-CuH1	1	TM ₃	0.37	1.4	22	≈0.1	0.2	6.0
	6	TM ₃	2.4	4.1	273	10	550	170
	16	TM ₁	*	*	3700*	1810	1200	8100

4.4 Holographic sensitivity

To compare the holographic sensitivity for modes of different samples, we determine the value of the holographic sensitivity R from the rate of hologram build-up in the initial stage,

$$R = \Delta(\sqrt{\eta})/\Delta(P_{\text{in}}\tau)|_{t \rightarrow 0}. \quad (5)$$

Here R depends strongly on input power P_{in} , and we can describe this behavior with a good accuracy by the relation

$$R = R_l + R_q P_{\text{in}}. \quad (6)$$

The obtained values of R_l and R_q are summarized in Table 2. The size of the ratio R_q/R_l is a measure for the contribution of two-photon processes to holographic recording. In Cu(I)-exchanged waveguides this ratio is about 0.43 W^{-1} , and this value remains constant after annealing of the samples. On the other hand, the same ratio in the Cu(II)-exchanged waveguides strongly decreases during annealing treatment: for the sample II-CuH1 annealed for 1 or 6 h, the ratio is about 46 W^{-1} , and after annealing for 16 h the value is decreased to 6.6 W^{-1} . This points to a principal transformation of the photorefractive centers at strong annealing of the Cu(II)-exchanged waveguides. Furthermore, from the experimental data we can conclude that the quadratic part of R is almost proportional to the Cu-related absorption.

5. Conclusions

By an additional Cu exchange the photorefractive properties of annealed proton-exchanged LiTaO₃ waveguides are considerably improved: the steady-state value of diffraction efficiency of holographic gratings in the waveguides is increased from 0.005 to 81%. We find a strong difference between Cu(I)-exchanged and Cu(II)-exchanged waveguides concerning 1. the spectral dependence of the Cu-related absorption, 2. the changes of the effective refractive indices, and 3. the photorefractive properties. This points to a crucial influence of the valence state of the Cu centers in the waveguides. A strong dependence of the photorefractive properties of the Cu:H:LiTaO₃ waveguides

on annealing time is found. A transformation of the valence state of Cu complexes in the Cu(II)-exchanged waveguides during annealing is discovered. Limitations of the maximum values of both, diffraction efficiency and holographic sensitivity, are caused by strong absorption and beam fanning. The ability to vary the photorefractive properties enables the optimization of a waveguide for a given application.

Acknowledgements We thank E. Krätzig for helpful discussions throughout these investigations and the DAAD (Deutscher Akademischer Austauschdienst) and DFG (Deutsche Forschungsgemeinschaft, SFB 225) for financial support.

References

- [1] S.M. KOSTRITSKII, D. KIP, and E. KRÄTZIG, *Appl. Phys. B* **65**, 514 (1997).
- [2] S.M. KOSTRITSKII, D. KIP, and E. KRÄTZIG, *Proc. Topical Meeting Photorefractive Materials, Effects, and Devices, Opt. Soc. Jpn., Waseda University, 1997* (p. 216).
- [3] V.E. WOOD, P.J. CRESSMAN, R.L. HOLMAN, and C.M. VEBER, *Topics Appl. Phys.* **61**, 45 (1989).
- [4] V.V. ATUCHIN and S.M. KOSTRITSKII, *Optoelectr. Instrum. and Data Process. No. 2*, 34 (1997).
- [5] F. RICKERMANN, D. KIP, B. GATHER, and E. KRÄTZIG, *phys. stat. sol. (a)* **150**, 763 (1995).
- [6] S.M. KOSTRITSKII and O.M. KOLESNIKOV, *J. Opt. Soc. Amer.* **B11**, 1674 (1994).
- [7] S.M. KOSTRITSKII, *J. Nonl. Opt. Phys. and Mater.* **6**, 321 (1997).
- [8] Y.A. BOBROV, V.A. GANSHIN, V.S. IVANOV, Y.N. KORKISHKO, and T.V. MOROZOVA, *phys. stat. sol. (a)* **123**, 317 (1991).
- [9] L.A. KAPPERS, K.L. SWEENEY, L.E. HALIBURTON, and J.H.W. LIAW, *Phys. Rev. B* **31**, 6792 (1985).
- [10] C.C. ZILING, V.V. ATUCHIN, I. SAVATINOVA, and M. KUNOVA, *Internat. J. Optoelectr.* **7**, 519 (1992).
- [11] H. AHLFELDT, J. WEBJORN, P.A. THOMAS, and S.J. TEAT, *J. Appl. Phys.* **77**, 4467 (1995).
- [12] R.E. HADI, P. BALDI, S. NOUH, M.P. DE MICHELI, A. LEYCURAS, V.A. FEDOROV, and Y.N. KORKISHKO, *Opt. Lett.* **20**, 1698 (1995).
- [13] N. UCHIDA, *J. Opt. Soc. Amer.* **63**, 280 (1973).
- [14] V. LEYVA, A. AGRANAT, and A. YARIV, *J. Appl. Phys.* **67**, 7162 (1990).
- [15] J.-J. LIU, P.P. BANERJEE, and Q. WANG SONG, *J. Opt. Soc. Amer.* **B11**, 1688 (1994).
- [16] T. FUJIWARA, X.F. CAO, and R.V. RAMASWAMY, *Proc. IEEE Trans. Automatic Control* **5**, 1062 (1994).
- [17] Y. KONDO and Y. FUJII, *Jpn. J. Appl. Phys.* **34**, L309 (1995).
- [18] T. FUJIWARA, R. SRIVASTAVA, X. CAO, and R.V. RAMASWAMY, *Opt. Lett.* **18**, 346 (1993).
- [19] M.M. HOWERTON and W.K. BURNS, *J. Lightwave Technol.* **10**, 142 (1992).